Keck All Sky Precision Adaptive Optics Program Overview

P. Wizinowich^a, J. R. Lu^b, S. Cetre^a, J. Chin^a, C. Correia^a, J-R. Delorme^a, L. Gers^a, S. Lilley^a, J. Lyke^a, E. Marin^a, S. Ragland^a, P. Richards^a, A. Surendran^a, E. Wetherell^a, C.-F. Chen^d, D. Chu^d, T. Do^d, C. Fassnacht^e, M. Freeman^b, A. Gautam^d, A. Ghez^d, L. Hunter^c, T. Jones^e, M. C. Liu^f, D. Mawet^g, C. Max^c, M. Morris^d, M. Phillips^f, J.-B. Ruffio^g, N.-E. Rundquist^h, S. Sabhlok^h, S. Terry^b, T. Treu^d, S. Wright^h

^aW. M. Keck Observatory

^bUniversity of California Berkeley

^cUniversity of California Santa Cruz

^cUniversity of California Santa Cruz ^dUniversity of California Los Angeles ^eUniversity of California Davis ^fUniversity of Hawaii ^gCalifornia Institute of Technology ^hUniversity of California San Diego

ABSTRACT

We present the status and plans for the Keck All sky Precision Adaptive optics (KAPA) program. KAPA includes (1) an upgrade to the Keck I laser guide star adaptive optics (AO) facility to improve image quality and sky coverage, (2) the inclusion of AO telemetry-based point spread function estimates with all science exposures, (3) four key science programs, and (4) an educational component focused on broadening the participation of women and underrepresented groups in instrumentation. For this conference we focus on the KAPA upgrades since the 2020 SPIE proceedings¹ including implementation of a laser asterism generator, wavefront sensor, real-time controller, asterism and turbulence simulators, the laser tomography system itself along with new operations software and science tools, and modifications to an existing near-infrared tip-tilt sensor to support multiple natural guide star and focus measurements. We will also report on the results of daytime and on-sky calibrations and testing.

Keywords: adaptive optics, laser tomography, near-infrared sensing, PSF reconstruction

1. INTRODUCTION

Thanks to funding from the NSF Mid-Scale Innovation Program the W.M. Keck Observatory (WMKO) embarked on a major new five-year AO initiative as of September 2018. KAPA consists of four key science programs, an upgrade to the Keck I AO facility² and an education program.

The key science programs are focused on the following challenges:

- 1. Constraining dark matter, the Hubble constant, and dark energy via strong gravitational lensing
- 2. Testing General Relativity and studying supermassive black hole interactions at the Galactic Center
- 3. Characterizing galaxy kinematics and metallicity using rare highly magnified galaxies
- 4. Directly studying gas-giant protoplanets around the youngest stars

Additional funding to support these science programs, and the associated science tool development, has been provided by the Gordon and Betty Moore Foundation.

The KAPA education program has elements ranging from undergraduate to post-graduate level with an overall goal of broadening participation in instrumentation for women and underrepresented minorities. Funding for the associated AstroTech summer instrumentation workshop has been provided by the Heising-Simons Foundation.

The goal of the KAPA upgrade is to improve the image quality delivered to the science instrument, OSIRIS³, with greater sky coverage, and to improve the quantitative science results by providing point spread function (PSF) estimates with each science exposure. OSIRIS is a near-infrared integral field spectrograph and imager. The elements

of the KAPA upgrade are illustrated in Figure 1. The physical location of the KAPA components with the Keck I AO system is shown schematically in Figure 2.

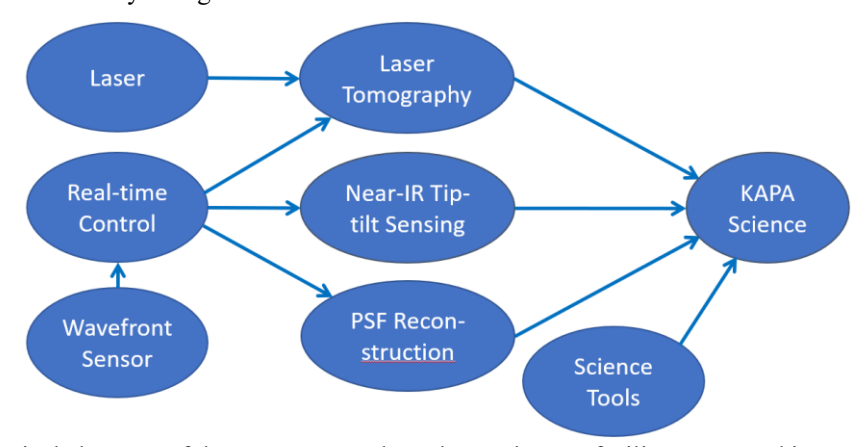


Figure 1: The technical elements of the KAPA upgrade to the Keck I AO facility. Improved image quality is provided by the laser tomography system, greater sky coverage via near-IR sensing, and improved quantitative science through PSF reconstruction.

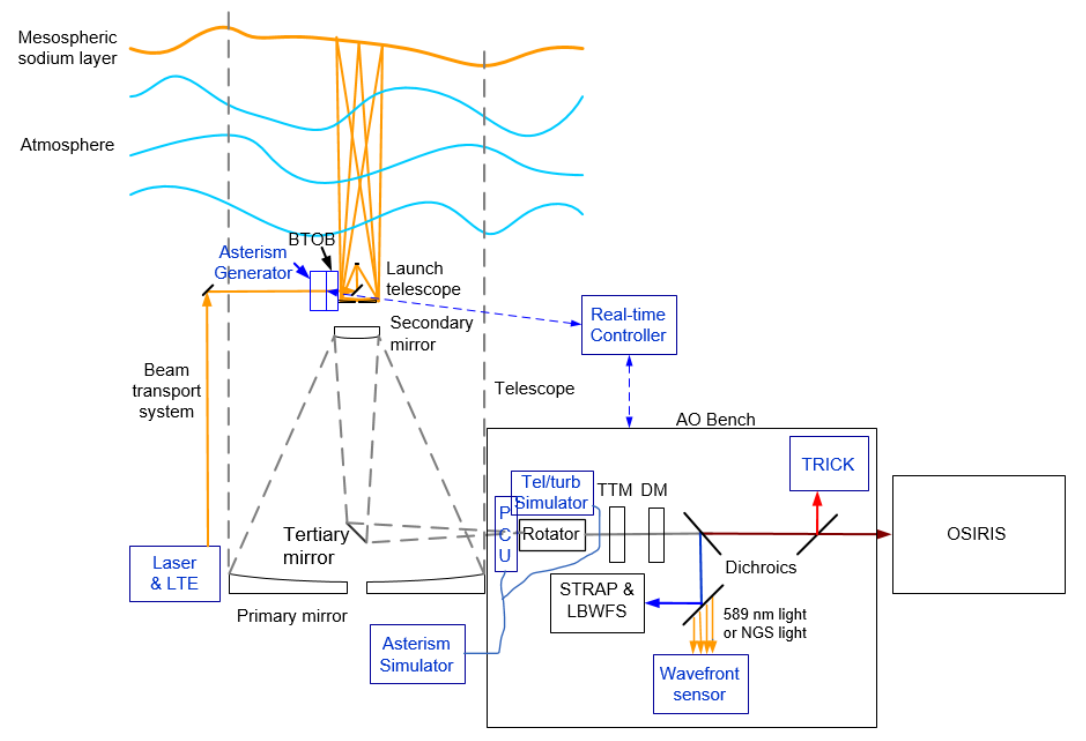


Figure 2: Location of KAPA related hardware (identified in blue text). The new laser head and laser table enclosure (LTE; providing laser formatting and diagnostics) are mounted on the telescope elevation ring with the laser electronics and supporting control systems in an enclosure on the right Nasmyth platform. The laser asterism generator is located just before the beam transfer optics bench (BTOB) mounted to the laser launch telescope behind the Keck telescope secondary mirror. The AO bench and OSIRIS science instrument are in an enclosure on the left Nasmyth platform. The new wavefront sensor camera and near-infrared tip-tilt sensor (TRICK) are mounted on the AO bench. Testing and calibration are supported by an asterism simulator source box in the AO electronics room that feeds optical fibers to the precision calibration unit (PCU; a 3-axis positioning stage) located at the input focal plane of the AO system and to a telescope/turbulence simulator whose output is folded along the AO optical axis by a fold mirror on the PCU. The RTC interface module is located in the AO electronics room with the RTC compute engine and telemetry server in the computer room off the Keck telescope.

The overall schedule approach has been to sequentially deliver science improvements on route to the full KAPA system, beginning with the new laser and real-time controller (RTC) required to support laser tomography. A TOPTICA/MPBC laser, identical to the laser previously implemented on Keck II,⁴ has been implemented to replace the Keck I LMCT laser. The new RTC is currently being commissioned on Keck I (an identical system is being implemented on Keck II with NSF MRI funding).⁵ The RTC upgrade includes a new larger format, lower noise wavefront sensor camera (OCAM2K).

The laser tomography system will use multiple laser guide stars (LGS) to reduce the "cone" effect. The laser tomography upgrade includes four components: a modification to the laser beam transport system to produce four LGS (the asterism generator), a modification to the wavefront sensor camera optics to sense all four LGS on the same detector, RTC modifications to support four LGS and a laser tomography algorithm, and an LGS asterism simulator system to support daytime calibration and testing. These hardware systems have been fabricated and integration at the telescope has begun with the plan to begin laser tomography daytime calibration and testing in the fall of 2023.

A near-infrared tip-tilt sensor⁸ will be extended to include focus sensing⁹ by early 2023. We will also be extending our NIRC2 PSF-reconstruction (PSF-R) approach^{10,11} to multiple LGS and OSIRIS in 2024.

Sections 2 to 8 follow the sequence shown in Figure 1. The error budget and predicted performance is discussed in section 9, followed by the education program in section 10. The final two sections are next steps and conclusions.

2. LASER GUIDE STAR FACILITY

As part of KAPA, the previous LMCT solid-state laser was replaced with a TOPTICA/MPBC Raman-fiber amplifier laser for higher sodium return (by a factor of 10 to allow multiple laser guide stars), higher reliability and lower maintenance. The new laser facility, including some beam train modifications, has been in science operation since May 2020. The on-sky laser performance is quite similar to that for the Keck II laser.⁴

3. WAVEFRONT SENSOR

The Shack-Hartmann wavefront sensor modifications for KAPA include new field stops, new pupil relay optics for four LGS, new reducer optics to relay the lenslet focal plane to the detector, and an OCAM2K camera. In NGS or single LGS mode only one of the four pupil relays will be used. The OCAM2K camera with reducer optics are in use with the new RTC. The new pupil relay optics will be installed after the new RTC is commissioned for science operations.

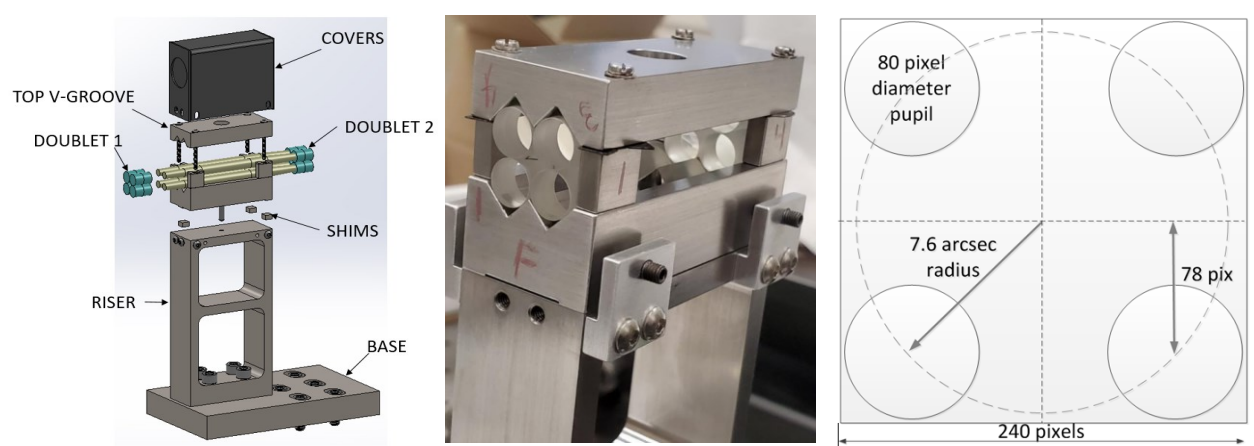


Figure 3: CAD model (left) and assembled (center) pupil relay opto-mechanics which produce four \sim 4 mm diameter images of the telescope pupil on an array of 0.2 mm square lenslets, one for each LGS on a 7.6" radius. The lenslet focal plane is relayed to the detector with a magnification of 0.48 (4x4 pixels/lenslet) by new reducer optics mounted to the front of the OCAM2k camera. The resultant pupil illumination on the OCAM2k detector is shown at right.

4. REAL-TIME CONTROLLER

The RTC⁵ has been developed by a consortium led by Microgate, including Swinburne University of Technology, Australian National University, and Observatoire de Paris, with expertise in the areas of hardware systems and controls, GPU computing, AO and simulations. The Keck I and II RTC's have been installed and are undergoing integration and test; a third (spare) RTC remains at the vendors to support testing.

The RTC architecture is shown in Figure 4. Microgate (consortium) is responsible for delivering the interface module (IM), computational engine (CE), and telemetry recorder server (TRS). The Keck I and II AO systems have eleven science modes requiring the RTC to be capable of interfacing with the Shack-Hartmann sensor (using the current SciMeasure camera or new OCAM2K camera), the near-infrared pyramid wavefront sensor (PWS), the near-infrared tip-tilt sensor (TRICK), the STRAP tip-tilt sensor, the Xinetics deformable mirror, and the downlink (DTT) and uplink (UTT) tip-tilt mirrors. It will also interface with a MEMS DM on Keck II and four additional UTT mirrors on Keck I. To reduce the footprint and impact of the RTC, only the IM is located near the AO optics bench. A fiber link capable of 40 GbE transfers both the sensor data to the CE and command data from the CE. This allows the CE and the TRS to be co-located in the temperature controlled computer room.

The CE is a Linux Server based on the CACAO (Compute and Control for AO) architecture of low latency, shared memories, and semaphores. The CE is based on NVidia's TESLA V100 TESLA boards with the CUDA development environment. Two VT100 TESLA boards are used for the CE; one for the real-time computer and one to support functionalities such as PSF-R, sensor fusion and predictive control. The second VT100 also provides redundancy in case of GPU failure. Raw and processed data are stored onto a 100TB TRS with 12 nights of capacity in the most data intensive mode.

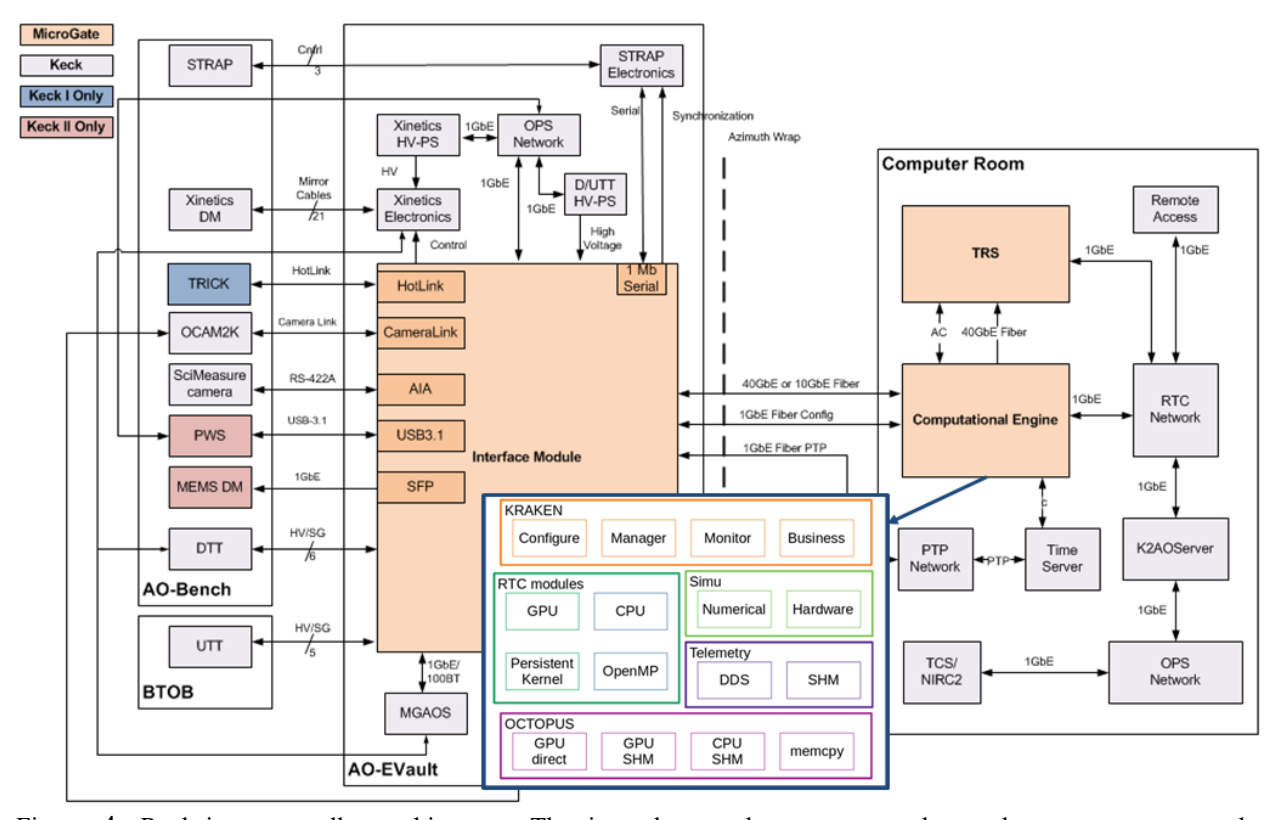


Figure 4: Real-time controller architecture. The inset box at bottom-center shows the components on the Computational Engine.

Within the CE, the software architecture uses modules such as KRAKEN (high level sequencing and user interface) and OCTOPUS (interface to shared memory) to configure the software and pass data directly to/from the GPUs. These modules, along with the layout of the business units (BUs), provide the user flexibility to modify or add algorithms for future needs. The use of semaphores, persistent kernels, shielding and direct memory transfers of data to the GPUs

provides low latency ($< 250 \mu s$) and jitter performance meeting the KAPA timing requirements. The COMPASS simulator framework is used to support simulation and analysis of the various modes.

5. LASER TOMOGRAPHY

4.1 Asterism Radius

Four LGS on an equilateral triangle with a 7.6" radius will be used for KAPA laser tomography. The number of LGS and radius were selected based on a combination of simulations and what radius would fit on the OCAM2K wavefront sensor camera. The predicted high order wavefront error versus zenith angle is shown in Figure 5.

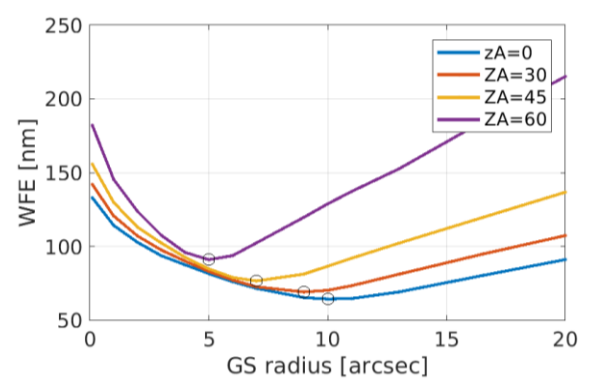
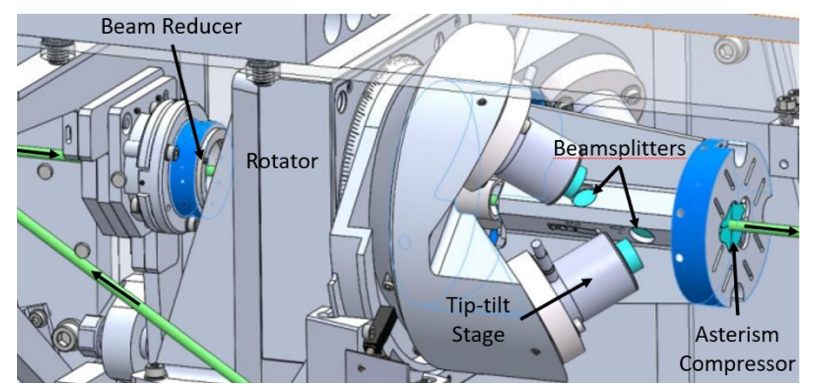


Figure 5: High-order wavefront error (tip-tilt removed) for median seeing conditions as a function of the guide star (GS) asterism radius (4 LGSs on a square) and ZA. The minima are indicated with black circles – almost perfect evolution with 1/airmass.

4.2 Asterism Generator

The asterism generator (AG) produces four LGS asterism from a single input laser beam as shown in Figure 6.⁶ The AG is located in the secondary module of the telescope as shown in Figure 7, \sim 2 m of optical path before the laser launch telescope. The four LGS are designed to be on a radius of 7.6" as they leave the launch telescope. Fast tip-tilt stages for each LGS provide up-link tip-tilt control based on the tip-tilt measured by the wavefront sensor. The AG assembly was fabricated by OMP Inc. in Canada.



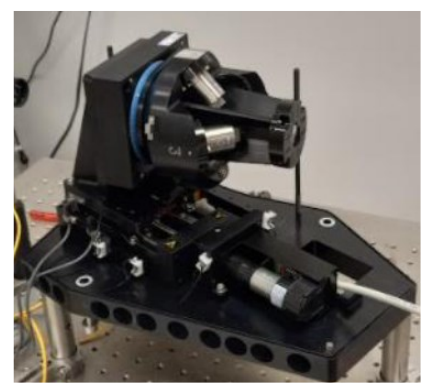


Figure 6: LGS asterism generator (AG). Left: CAD model. The laser (green beam) passes through a doublet to reduce the beam diameter to prevent vignetting in the subsequent opto-mechanics. The AG is mounted on a rotator to allow the asterism to be fixed on sky. The rotator is mounted on a translation stage to allow switching to single LGS mode. The AG consists of three beamsplitter cubes and a right angle prism each reflecting ¼ of the input light. Each of the resultant four beams reflects off a 25 mm diameter PI piezo actuated mirror used for up-link tip-tilt control. The onsky angle off each tip-tilt mirror is 7.6" toward the center axis. The compressor prisms act as a periscope to bring the beams closer together so they overlap at the launch telescope secondary mirror. Right: The as-built AG.

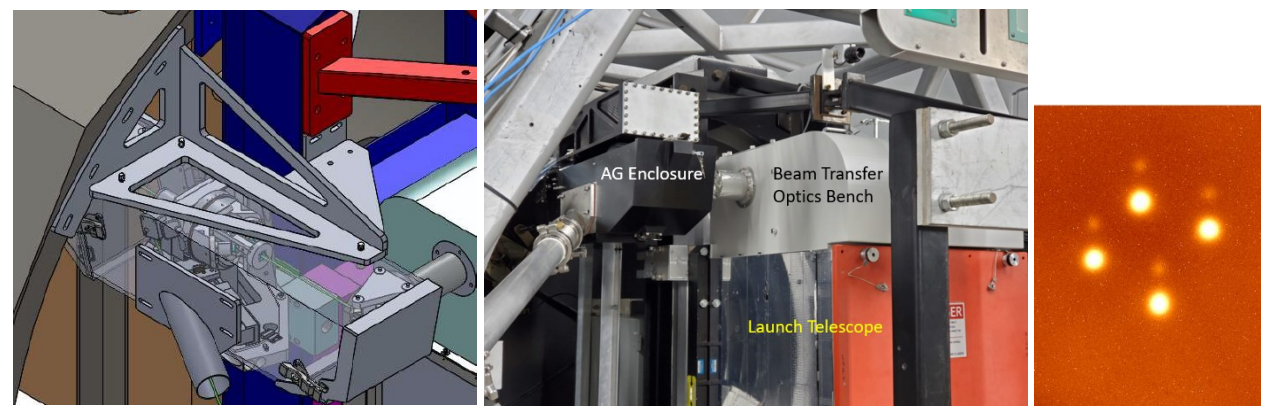


Figure 7: Left: Asterism generator enclosure, with a transparent view into the enclosure, mounted on the Keck telescope secondary mirror module. Center: Installed system. Right: Laser asterism on-sky imaged with the AO acquisition camera (the ghosts are from a beamsplitter in the acquisition camera path).

4.3 Daytime LTAO Calibration and Testing Infrastructure

This infrastructure will be used on the AO bench to calibrate the AO system and to perform daytime tests to understand, characterize and optimize the performance.⁷ In addition to the tools described below the new RTC will allow application of turbulence, at high rates, to the AO system's tip-tilt and deformable mirrors.

4.3.1 Asterism Simulator

The asterism simulator consists of a light source box and fibers going to the precision calibration unit (PCU¹²) and the telescope/turbulence simulator. Multi-mode fibers (~1" diameter) simulate the LGS using 590 nm light and multi-mode fibers. Single mode fibers, diffraction-limited at H and K-band, simulate the NGS using a broad-band source. Since they need to be used for visible tip-tilt sensing with STRAP, the single-mode fibers were chosen to be fluoride fibers having a near-uniform throughput from the R-band to the K-band. The LGS intensities can be individually controlled over a range of 4 magnitudes in the R-band, and the white light intensities can be varied over a magnitude of 10 over R to K bands. The source box is installed and in use at the telescope. The fiber chuck mounted to the PCU is shown in Figure 8.

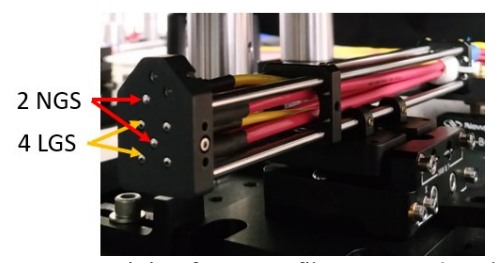


Figure 8: Fiber chuck mounted to the PCU containing four LGS fibers on a 7.6" radius, an on-axis science target NGS fiber and an off-axis NGS fiber (to be used for low order correction).

4.3.2 Precision Calibration Unit

From the LTAO perspective the PCU is used to position fibers in the AO bench input focal plane or to reflect light from the telescope and turbulence simulator to this input focal plane. The PCU has two additional functions: to insert a precision pinhole grid in the focal plane for science instrument distortion calibration and to insert a fold mirror that reflects telescope light to the Keck Planet Finder (KPF) fiber injection unit (FIU; the FIU is mounted on the AO bench).¹³ The PCU, shown in Figure 9, is installed and in use at the telescope.

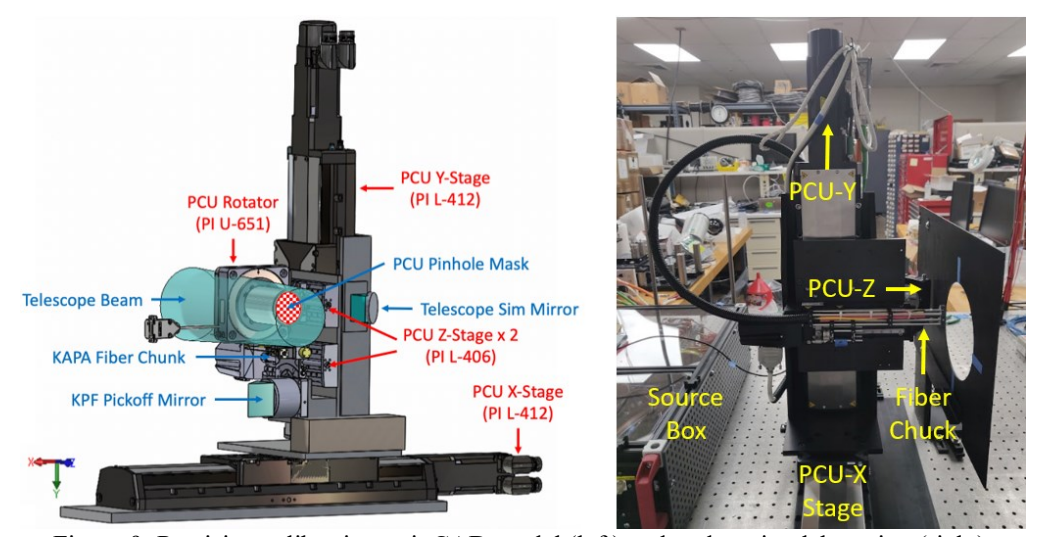


Figure 9: Precision calibration unit CAD model (left) and undergoing lab testing (right).

4.3.3 Telescope and Turbulence Simulator

A combined telescope and turbulence simulator has been developed that simulates an LGS asterism at 100 km altitude and an on-axis NGS at infinity, as shown in Figure 10. The telescope simulator consists of two identical achromats with a pupil mask, matching the Keck telescope pupil, located between them. The first lens collimates the light from the NGS source and the second lens reconverges the light with the same f/# and exit pupil as the Keck telescope. The simulator also includes an integrating sphere for OSIRIS calibrations; a manually installed fold mirror reflects the light from the integrating sphere through a pupil mask and the second achromat.



Figure 10: Partially assembled telescope and turbulence simulator system. The turbulence phase screen will be located between achromat 1 and the pupil mask; a fast translation stage simulates wind-driven turbulence by moving the phase screen perpendicular to the optical axis and a slow translation stage changes the turbulence altitude.

A phase screen, produced at the University of California at Santa Cruz, will be used to introduce turbulence at different wind speeds (up to 10 m/s) and altitudes (1 km to 12 km). The deformable mirror will be used to inject ground-layer turbulence. The phase screen is located between the first achromat and the pupil mask. The equivalent wind speed is achieved by translating the phase screen perpendicular to the optical axis; the travel range of this stage allows for a 2.2 s measurement (the phase screen is 2.5 times the diameter of the Keck pupil) at an equivalent wind speed of 10 m/s or a translation stage speed of 33 mm/s. The equivalent altitude is increased by moving the phase screen away from the pupil mask toward the first achromat. The equivalent altitude is the one where the LGS fiber's beam size and

off-axis distance is the same as at that altitude. The phase screen has a mean r_0 of 0.227 m in the telescope pupil computed from a tilt-removed fit to Noll's variances.

4.3.4 Daytime Testing and Calibration

The system-level daytime calibration and testing plan includes the following four phases as the tomography hardware and software are implemented with the AO system:

- 1. Deployment of the new asterism simulator and its usage for all the daytime tests and calibrations for the NGS and single LGS AO.
- 2. Deployment of the new telescope/turbulence simulator and its usage for daytime tests and calibrations, with the additional benefit of a telescope pupil. The turbulence altitude, wind speed and r₀ should be calibrated during this phase.
- 3. Integration, calibration and testing of the new pupil relay optics. The first step is to ensure these optics can be used to support NGS and single LGS AO science operations.
- 4. Laser tomography (LT) AO calibration and testing. This stage will include the development of tools to interface the telescope simulator to the AO bench and scripts to conduct performance assessment of closed-loop tomographic reconstruction on the bench.

All four phases include closed loop testing, including applying turbulence to the deformable mirror and tip-tilt mirror. Once Phase 3 is in place turbulence at altitude can be added to the closed loop testing.

4.4 Tomography Algorithm

The laser tomography algorithms are considerably different from the NGS and single LGS cases in that the advocated regulator is a pseudo open-loop controller (POLC) using a minimum mean-square error (MMSE) tomographic reconstructor. The latter is partially based on a model integrating both geometric system and statistical atmospheric parameters (seeing, Cn2 profile, structured noise from elongated LGS spots). The daytime calibration infrastructure will be essential in testing the performance of this model-based tomography algorithm, and how the deviations between real atmospheric conditions and the model can affect AO performance. The POLC consists of two major steps: tomographic reconstruction (spatial) and control (temporal filtering) – and can in principle drive all other AO modes, whether NGS or single LGS bringing full MMSE reconstruction to mainstream AO operation. The focal anisoplanatism error is predicted to be reduced from about 150 nm rms to the 80 nm rms level.

The RTC has been designed with considerable extra capacity and for programming flexibility. As part of a risk reduction exercise to ensure that the high-order loop will conform to the latency requirement of $<250\mu s$, a prototyping code consisting of the complete high order loop implementation was created to operate on a gaming GPU using Compute Unified Device Architecture (CUDA) and the associated CUDA Basic Linear Algebra Subprogram (CUBLAS) libraries. In addition to performance, this implementation was functionally compared with a CPU based implementation of the loop and representative dummy values for the WFS input pixels. The timing statistics for the high throughput, time critical stream had an average loop time of 60 μ s and a maximum loop time of 115 μ s over 50,000 frames. The POLC loop has an additional processing stream operated during the loop dead time (processes between the end of DM output and the availability of the next set of WFS data). The dead-time latency was found to be on average 21.39 μ s and a maximum of 33 μ s over the same set of frames.

6. NEAR-INFRARED TIP-TILT SENSOR

A near-infrared tip-tilt sensor is mounted to the AO bench just before OSIRIS and is fed by a choice of dichroic beamsplitters.⁸ This system has been in shared-risk science usage since late 2020. An example of the improved performance with this sensor (discussed elsewhere in this conference) is shown in Figure 11.¹⁵

The KAPA upgrade will include using this sensor for slow focus, and possibly astigmatism, measurements using the LIFT algorithm. Other plans include testing improved methods for system optimization, tip-tilt sensing (e.g. correlation), sky subtraction and using up to three NGS for tip-tilt sensing to reduce tip-tilt anisoplanatism.

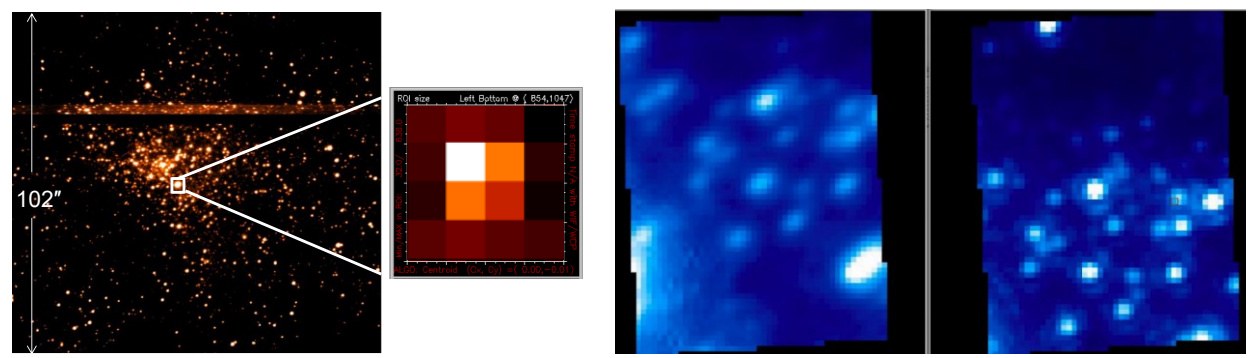


Figure 11: From left to right: (1) An image of the Galactic Center taken with the H2RG detector. (2) A 4x4 pixel (0.05" pixels) region of interest is read multiple times to reduce noise. (3) an OSIRIS integral field spectrograph image of the Galactic Center using the visible tip-tilt sensor and (4) the near-infrared tip-tilt sensor.

7. PSF RECONSTRUCTION

A multi-institutional point spread function reconstruction (PSF-R) development effort has been undertaken for science with NIRC2 on Keck II. 10,11 The NIRC2 tool includes an algorithm to reconstruct the on-axis PSF based on the AO telemetry, and algorithms to generate the off-axis components based on the measured instrument off-axis aberrations and atmospheric profiler data. The PSF-R estimates have been successfully demonstrated on-sky for point sources. However, the science verification efforts so far have had limited success. 16 The current AO telemetry-based PSF-R is challenged by the presence of significant unsensed residual wavefront aberrations, the need for on-sky phase diversity measurements and the potential presence of dynamic changes. The next step is to test some of the optical transfer function (OTF) terms of the PSF-R algorithm on the AO bench with simulated turbulence.

One of the logistical challenges for science verification is that the original on-axis PSF-R algorithm was written in IDL which requires an end-user license. To provide an open source for PSF reconstruction, a python-based software package, developed at the Laboratoire d'Astrophysique de Marseille, is being tested that captures the previous on-axis PSF-R development. The new tool should be easily usable by the observers, increasing the chances of independent PSF-R verification for the NIRC2 instrument. Subsequently, the PSF-R tools will be extended to the OSIRIS imager and integral field spectrograph for the standard modes of operation. For LTAO mode, we are exploring an alternative approach to a telemetry-based scheme besides adding additional OTF terms for laser tomography to the existing one.

Through other projects, there are efforts to understand and mitigate the residual wavefront aberrations in the Keck AO systems. An on-sky phase retrieval technique has been demonstrated and a residual wavefront controller system was proposed to optimize the AO system in real-time.¹⁷ Successful implementation of some of the optical and calibration effects identified in these efforts could reduce the residual aberration in the system, improving the performance of both Keck AO and PSF-R.

The nightly AO telemetry data will be processed by pipeline software to provide a grid of PSFs that are archived in the Keck Observatory Archive along with the science data. Some progress has been made to extend these tools for integral field spectroscopy with OSIRIS.

Progress on the AIROPA software package to model off-axis, AO PSFs and extract stellar astrometry and photometry, and test results using Keck NIRC2 images, is summarized elsewhere in this conference¹⁸ and in a series of future journal papers. ^{19,20,21}

8. KAPA SCIENCE

8.1. Science Programs

Beginning in late 2023, subsequent to commissioning of the upgraded system, each science program will perform 20 to 42 nights of science observations spread over three to five years. A number of legacy science products will be released and point spread function (PSF) estimates will be provided for each science exposure in the Keck Observatory Archive (KOA).

To ensure that the four KAPA science programs provide the community with a valuable scientific legacy, the data sets will be publicly released through the Keck Observatory Archive and the specific science products will be published.

The four science programs are led by Tommaso Treu (UCLA) for dark matter/energy; Andrea Ghez, Tuan Do and Mark Morris (UCLA) for the Galactic Center; Shelley Wright (UCSD), Tucker Jones (UCD) and Claire Max (UCSC) for galaxy evolution; and Michael Liu (UH) and Dimitri Mawet (Caltech) for gas-giant protoplanets. In addition, Jessica Lu (UCB) is the KAPA project scientist.

8.2. Science Tools

Along with the technical and instrumental upgrades that form the primary elements of KAPA, a suite of science tools is being developed. These tools are necessary for observers to plan observations and reduce data, and will be essential in the production of scientific results in each of the four KAPA science surveys. They will also be made broadly available to the Keck community to maximize the total scientific return of KAPA. These tools include:

- Performance Predictions for survey planning and requirements validation. KAPA PSFs have been provided for each science case.
- 2. Strehl ratio and FWHM Prediction Calculator, based on the performance predictions, has been provided at http://bhs.astro.berkeley.edu:8501/ for observation planning.
- 3. OSIRIS Exposure Time Calculator (ETC; https://oirlab.ucsd.edu/osiris/etc/) for observing planning and science requirements validation. The ETC uses KAPA PSFs and desired observational parameters to predict the SNR on the OSIRIS imager and integral field spectrograph.
- 4. *OSIRIS Simulator* for the KAPA PSFs through the OSIRIS imager and integral field spectrograph to support experimental design optimization.
- 5. OSIRIS Data Reduction Pipelines (DRPs) for the imager (https://github.com/Keck-DataReductionPipelines/KAI) and improving the existing integral field spectrograph DRP (https://www2.keck.hawaii.edu/inst/osiris/tools/index.php), including additional instrument performance characterization.
- 6. *OSIRIS Distortion Solution*. ¹² An on-sky distortion solution is in progress. The pinhole mask on the precision calibration unit will be used for daytime distortion calibrations in the future.
- 7. OSIRIS Field Dependent Imager Aberrations. The tools are being developed to characterize the field dependent aberrations as an important component of off-axis PSF reconstruction.
- 8. *End-to-end Simulations* will be developed by each science team for their science targets using the KAPA PSFs, including data reduction and science analysis, to determine the quantitative performance and to identify strategies to mitigate residual uncertainties.
- 9. System Health Monitoring procedures and/or pipelines to regularly monitor basic instrument calibrations, and long-term analysis for improved science team data extraction.

9. ERROR BUDGET AND PREDICTED PERFORMANCE

Detailed error budgets and PSF estimates have been developed for KAPA observations of targets representing each of the four key science programs. Two tools have been used to support the performance modeling: a detailed error budget excel spreadsheet and a Matlab-based physical optics simulation model (OOMAO).

The spreadsheet tool was anchored against the current Keck NGS and LGS AO nightly metric data and published Galactic Center data 22,23 . The spreadsheet tool's predicted results match the measured data very well as shown in Table 1. In order to achieve this match an additional high order term of 130 nm rms had to be added to all cases, and 6 mas rms of tip-tilt residual had to be added to the LGS AO cases. The former is believed to be largely due to primary mirror phasing errors that are unsensed or poorly sensed by the wavefront sensor. The terms that contribute > 30 nm rms of wavefront error to the LGS AO error budget are shown in Table 2.

Table 1: Summary table for the predicted performance in comparison with the measured performance. The last two columns show the high order (HO) and tip-tilt (TT) margins required to match the measured performance.

Case	λ	Strehl Ratio		FWHN	l (mas)	Margin		
Case		Meas	Pred	Meas	Pred	HO (nm)	TT (mas)	
Nightly NGS	K	0.53	0.53	50	50	130	0	
Nightly LGS	K	0.44	0.44	53	53	130	7	
Galactic Center	K	0.30	0.30	60	60	130	6	
	Н	0.16	0.17	64	64	130	0	

Table 2: High order and tip-tilt error terms contributing > 30 nm rms to the LGS AO error budget. The contributions of all terms, including those < 30 nm are included in the Total Error rows. KAPA is primarily designed to reduce the bandwidth error with the new RTC and the focal anisoplanatism error with LTAO. Other terms that are expected to be reduced as a result of KAPA include the HO wavefront error margin with improved primary mirror phasing (e.g. Figure 12) and the TT error margin through the use of the near-infrared tip-tilt sensor.

			Wavefront				Science Band	
Science High-order Errors (LGS Mode)				Error (rms)		Parameter		К
Atmospheric Fitting Error				nm	20	Subaps		•
Bandwidth Error				nm	24	Hz (-3db)		
High-order Measurement Error				nm	20	W		
High-Order Aliasing Error				nm	0.3	Fitting reduction factor		
LGS Focal Anisoplanatism Error				nm	1	sci beacon(s)		
Uncorrectable Static Telescope Aberrations				nm	20	Acts Across Pupil		
Uncorrectable Dynamic Telescope Aberrations				nm		Dekens Ph.D		
Dynamic WFS Zero-point Calibration Error				nm		Allocation		
Residual Na Layer Focus Change				nm	30	m/s Na layer vel		
DM Finite Stroke Errors				nm	4.0	um P-P stroke		
Uncorrectable AO System Aberrations				nm		Allocation		
Uncorrectable Instrument Aberrations				nm		NIRC2		
HO Wavefront Error Margin				nm		Allocation		
Total High Order Wavefront Error				nm	Strehl Ratio		0.32	0.50
Science Tip/Tilt Errors Angu		ular	Equiv	alent	Parameter			
		Error (rms)		WFE (rms)		Parameter		
Residual Telescope Wind Shake Jitter (one-axis)		mas	44	nm	29	Hz input disturbance		
TT Error Margin		mas	116	nm	Allocation			
Total Tip/Tilt Error (one-axis)		mas	119	nm		Strehl Ratio	0.87	0.89
Total Effective Wavefront Error	315		Strehl Ratio		0.28	0.44		
Total Effective wavefront Error				nm		FWHM (mas)	48.3	52.5

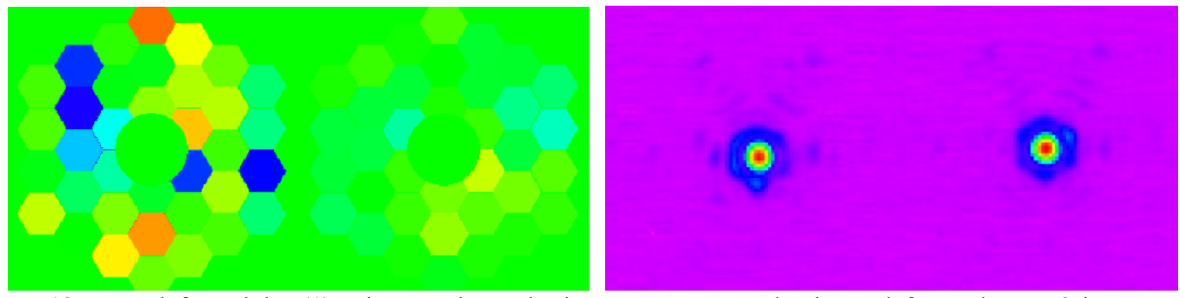


Figure 12: From left to right: (1) Primary mirror phasing errors measured using a defocused NIRC2 image and a Gerchberg-Saxton phase retrieval algorithm with segment constraints.^{24,25} (2) Phasing errors after applying corrections to the primary mirror active control system. An in-focus star image on NIRC2 before (3) and after (4) applying the

correction. The segment piston errors were reduced from 124 nm to 23 nm rms and the Strehl ratio was improved from 56% to 61%.

The Galactic Center current and predicted performance with the RTC and full KAPA upgrades, including using one bright nearby star on the near-infrared tip-tilt sensor (TRICK), are shown in Figure 13 under median conditions. KAPA is predicted to achieve a high order wavefront error of 244 nm rms with a residual tip-tilt error of 5.6 mas rms on-axis resulting in an H-band Strehl ratio of 0.36 (versus 0.16 currently), and ~50% ensquared energy in a 50 mas integral field spectrograph aperture. Figure 14 provides plots of Strehl ratio and FWHM versus field position from the physical optics simulation model. The resultant PSFs versus field position are provided to the science team for science analysis.

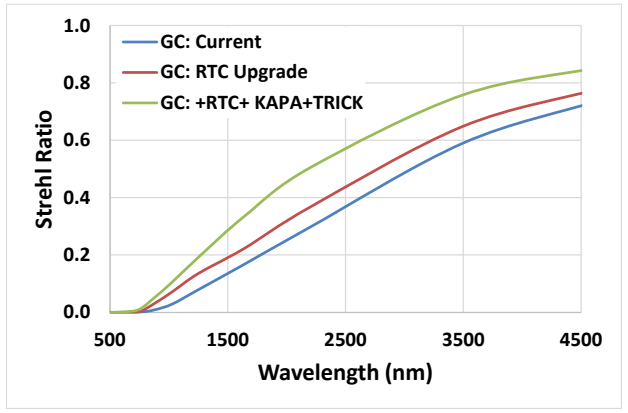


Figure 13: Current (blue) and predicted Galactic Center performance for the RTC (red) and KAPA (green) upgrades.

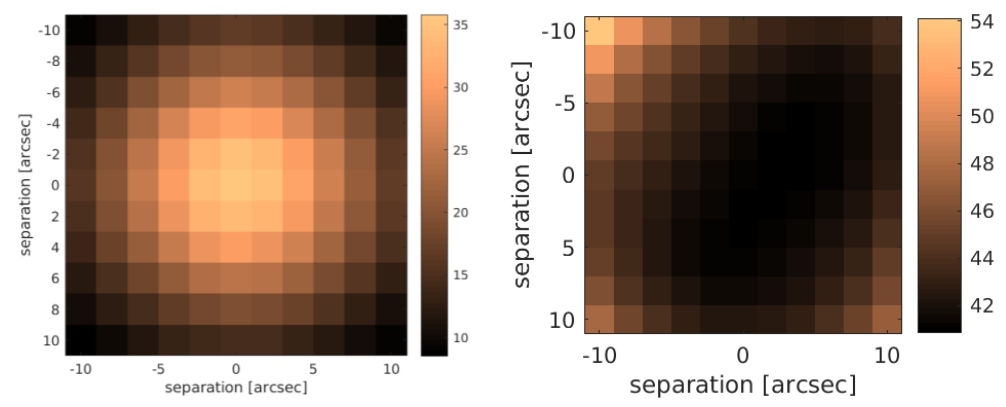


Figure 14: Galactic Center H-band Strehl ratio (left) and FWHM maps for KAPA in median seeing conditions.

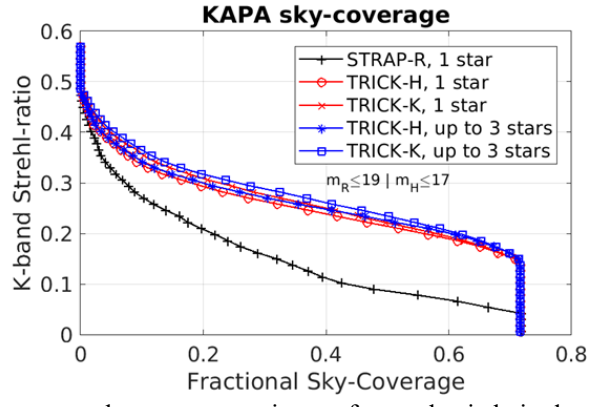


Figure 15: K-band Strehl ratio versus sky coverage estimates for a galactic latitude of 60°, longitude of 0°, and zenith angle of 30°, using STRAP, or TRICK in H- or K-band.

For a sample lensed galaxy target the predicted H-band performance is a 0.37 Strehl ratio and 44 mas FWHM, using three near-infrared tip-tilt stars on TRICK, versus the current performance of 0.23 and 53 mas using one visible tip-tilt star on STRAP.

KAPA's predicted sky coverage (for galactic latitude 60°, longitude 0°, and 30° zenith angle) is shown in Figure 15. There is no statistical gain in using more than one tip-tilt star, however there would likely be gains for some specific science cases.

10. EDUCATION PROGRAM

The overall goal of the KAPA education program is to broaden participation in astronomical instrumentation to include more women and underrepresented minorities. This program (see Figure 16) includes hosting scholars through the Akamai (for Hawaii undergraduate students) and Keck Visiting Scholars (KVS) programs, developing a new one-week instrumentation summer school called AstroTech funded by the Heising-Simons Foundation led by Lisa Hunter and Jessica Lu, and employing about eight KAPA science postdocs and a KAPA technology postdoc.

Through August 2022 student involvement will have included:

- Four Akamai students, one non-Akamai undergraduate, two KVS and a three-year KAPA technical postdoc have been engaged in KAPA projects at Keck Observatory.
- KAPA science postdocs at UCLA (three), UCB (two), UCSD (one) and UH (one).
- AstroTech summer schools held in 2019, 2021 and 2022 (https://isee-telescope-workforce.org/astrotech/). The 2021 student cohort of 25, selected from a total of 118 applicants, included 84% women and 36% underrepresented minorities from 20 different institutions across the U.S.

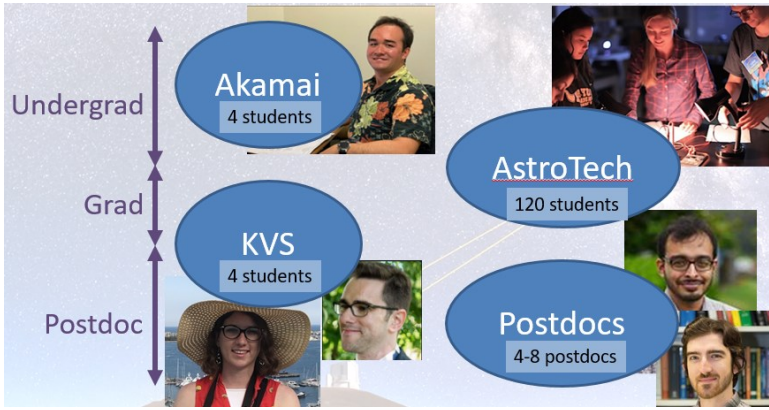


Figure 16: KAPA education program designed to broaden participation in instrumentation for women and underrepresented minorities.

11. NEXT STEPS

The KAPA project is behind schedule due to a combination of factors, many stemming from Covid impacts and some of which are still being experienced by the project and observatory. Up to a one-year extension beyond the nominal completion date of the end of August 2023 will likely be required to complete the KAPA science verification. The key remaining technical development milestones are summarized in Table 3.

Table 3: Key remaining KAPA technical milestones.

Key Milestone	Completion Date	
Daytime Tomography Calibration System Operational	Sep-22	
Real-time Controller (RTC) demonstrated for NGS Science	Sep-22	
Laser Asterism Operational	Nov-22	
RTC demonstrated for LGS Science	Dec-22	
Daytime Tomography Systems Integrated	Dec-22	
RTC and Wavefront Sensor Operations Handover	Jan-23	
Focus Algorithm Operational with Near-IR Sensor	Jan-23	
RTC & Wavefront Sensor Tomography Upgrades Integrated	Apr-23	
On-sky Tomography Demonstrated	Jun-23	
On-sky Tomography Performance Characterized	Sep-23	
Tomography Operations Handover	Oct-23	
NGS/LGS PSF-R Algorithm Sky Tested	Oct-23	
Laser Tomography PSF-R Algorithm Sky Tested	Jul-24	

12. CONCLUSION

The five-year KAPA program will upgrade the Keck I AO system with a new higher return sodium-wavelength laser, a new real-time controller for higher bandwidth and increased capacity to support both KAPA and future upgrades, multiple LGS for laser tomography, extended sky coverage with near-infrared low order sensing, and PSF-R for quantitative KAPA science observations with OSIRIS. The AO correction and sky coverage are predicted to be significantly improved as a result. The resultant KAPA system will be used to carry out four key science programs as well as supporting all science observations with the Keck I AO system. A suite of science tools is being developed to support observation planning and data analysis. An extensive education program is in place and has been integrated with KAPA technical developments where possible.

13. ACKNOWLEDGEMENTS

The W. M. Keck Observatory is operated as a scientific partnership among the California Institute of Technology, the University of California, and the National Aeronautics and Space Administration. The Observatory was made possible by the generous financial support of the W. M. Keck Foundation. The authors wish to recognize and acknowledge the very significant cultural role and reverence that the summit of Maunakea has always had within the indigenous Hawaiian community. We are most fortunate to have the opportunity to conduct observations from this mountain. Funding support for the KAPA system is provided by the National Science Foundation Mid-Scale Innovations Program award AST-1836016 (PI: Wizinowich). The Keck II real-time controller is funded by the NSF Major Research for Instrumentation Program award AST-1727071 (Wizinowich). Funding support for the KAPA science programs is provided by the Gordon and Betty Moore Foundation through awards to UH (Liu), UCSD (Wright) and two awards to UCLA (Ghez and Treu), and sub-awards to CIT (Mawet), UCB (Lu) and UCD (Jones). Funding support for the AstroTech instrumentation intensive is provided by the Heising-Simons Foundation through UCSC (Hunter) and UCB (Lu). The turbulence simulator was supported by a grant from R. Simperman. The precision calibration unit was supported by a UCO mini-grant and NSF award AST-2108015 (Lu). Finally, we would like to acknowledge our external technical reviewers and collaborators for their assistance: A. Boucher, C. Boyer, M. van Dam, R. Dekany, S. Esposito, T. Fusco and J.-P. Veran.

REFERENCES

- [1] Wizinowich, P., et al., "Keck All Sky Precision Adaptive Optics," Proc. SPIE 11448-0E (2020).
- [2] Chin, J., et al., "Keck I Laser Guide Star Adaptive Optics System," Proc. SPIE 8447 (2012).
- [3] Larkin, J., et al., "OSIRIS: A diffraction limited integral field spectrograph for Keck," New Astronomy Reviews 50 (2006)
- [4] Chin, J., et al., "Keck II laser guide star adaptive optics system and performance with the TOPTICA/MPBC laser," Proc. SPIE 9909 (2016).
- [5] Chin, J., et al. "Keck adaptive optics facility: real-time controller upgrade," Proc. SPIE 12185 (2022).
- [6] Lilley, S., et al. "An asterism generator for Keck All Sky Adaptive Optics," Proc. SPIE 12185 (2022).

- [7] Surendran, A., et al. "Daytime calibration and testing of the Keck All Sky Precision Adaptive Optics tomography system." Proc. SPIE 12185 (2022).
- [8] Femenia-Castella, B., et al., "Status and new developments with the Keck I near-infrared tip-tilt sensor," Proc. SPIE 9909 (2016).
- [9] Plantet, C., et al., "LIFT on Keck: analysis of performance and experiments towards on-sky validation," AO4ELT5 (2017).
- [10] Ragland, S., et al., "Status of Point Spread Function Determination for Keck Adaptive Optics," Proc. SPIE 10703 (2018).
- [11] Beltramo-Martin, O., et al., "PRIME: PSF Reconstruction and Identification for Multiple-source characterization Enhancement application to Keck NIRC2 imager," MNRAS 487, 5450 (2019).
- [12] Freeman, M., et al., "An optical distortion solution for the Keck I OSIRIS imager," Proc. SPIE 12185 (2022).
- [13] Lilley, S., et al., "A fiber injection unit for the Keck Planet Finder," Proc. SPIE 12184 (2022).
- [14] Correia, C., et al., "Static and predictive tomographic reconstruction for wide-field multi-object adaptive optics systems," JOSA A 31, 101 (2014).
- [15] Chu, D., et al., "Evaluating the performance of the Keck Observatory adaptive optics systems on crowded field data using different adaptive optics configurations," Proc. SPIE 12185 (2022).
- [16] Chen, G., et al., "Point spread function reconstruction of adaptive-optics imaging: meeting the astrometric requirements for time-delay cosmography," MNRAS 508, 755 (2021).
- [17] Ragland, S. et al., "Residual Wavefront Control of Segmented Mirror Telescopes," Proc. SPIE, 12185 (2022).
- [18] Lu, J., et al., "AIROPA: Off-axis Adaptive Optics PSF Reconstruction in Simulation, On-bench, and On-sky," Proc. SPIE 12185-145 (2022).
- [19] Ciurlo, A., et al., AIROPA II: Modeling Instrumental Aberrations for Off-Axis Point Spread Functions in Adaptive Optics," JATIS (submitted, 2022).
- [20] Turri, P., et al., "AIROPA III: Testing Simulated and On-Sky Data," JATIS (submitted, 2022).
- [21] Terry, S., et al., "AIROPA IV: Validating Point Spread Function Reconstruction on Various Science Cases," in preparation (2022).
- [22] Jia, S., et al. "The Galactic Center: Improved Relative Astrometry for Velocities, Accelerations and Orbits near the Supermassive Black Hole," ApJ 873, 9J (2019).
- [23] Do, T., et al., "Relativistic redshift of the star S0-2 orbiting the Galactic Center supermassive black hole," Science 365, 644D (2019).
- [24] Ragland, S., "A Phase Retrieval Technique to Measure and Correct Residual Segment Piston Errors of Large Aperture Optical Telescopes," Proc. SPIE 12182, 12182-8 (2022).
- [25] van Kooten, M., et al. "On-sky reconstruction of Keck Primary Mirror Piston Offsets using a Zernike Wavefront Sensor," ApJ 932, 109V (2022).